European Radiology (2019) 29:963–974
https://doi.org/10.1007/s00330-018-5633-6

CARDIAC

# Assessment of Cardiac Lead Perforation: Comparison Among Chest Radiography, Transthoracic Echocardiography and Electrocardiography-gated Contrast-enhanced Cardiac CT

Xiang Zhang[1] · Chushan Zheng[1] · Peiwei Wang[2] · Dongye Wang[1] · Boshui Huang[2,3] · Guozhao Li[1] · Huijun Hu[1] · Zehong Yang[1] · Xiaohui Duan[1] · Shaoxin Zheng[2] · Pinming Liu[2,3] · Jingfeng Wang[2,3] · Jun Shen[1]

Received: 24 May 2018 / Revised: 19 June 2018 / Accepted: 26 June 2018 / Published online: 17 July 2018


## Abstract

**Objectives** Cardiac lead perforation is a rare but potentially life-threatening event. The purpose of this study was to investigate the diagnostic performances of chest radiography, transthoracic echocardiography (TTE) and electrocardiography (ECG)-gated contrast-enhanced cardiac CT in the assessment of cardiac lead perforation.

**Methods** This retrospective study was approved by the ethics review board of Sun Yat-Sen Memorial Hospital at Sun Yat-Sen University (Guangzhou, China), and the need to obtain informed consent was waived. Between May 2010 and Oct 2017, 52 patients were clinically suspected to have a cardiac lead perforation and received chest radiography, TTE and ECG-gated contrast-enhanced cardiac CT. Among them, 13 patients were identified as having cardiac lead perforation. The diagnostic performances of these three modalities were evaluated by receiver-operating characteristic (ROC) curves using a composite reference standard of surgical and electrophysiological results and clinical follow-up. The areas under ROCs (AUROCs) were compared with the McNemar test.

**Results** The accuracies of chest radiography, TTE and ECG-gated contrast-enhanced cardiac CT imaging for the diagnosis of cardiac lead perforation were 73.1%, 82.7% and 98.1%, respectively. ECG-gated contrast-enhanced cardiac CT had a higher AUROC than chest radiography ($p < 0.001$) and TTE ($p < 0.001$).

**Conclusions** ECG-gated contrast-enhanced cardiac CT is superior to both chest radiography and TTE imaging for the assessment of cardiac lead perforation.

**Key Points**

- *ECG-gated contrast-enhanced cardiac CT has an accuracy of 98.1% in the diagnosis of cardiac lead perforation.*
- *The AUROC of ECG-gated contrast-enhanced cardiac CT is higher than those of chest radiography and TTE imaging.*
- *ECG-gated contrast-enhanced cardiac CT imaging has better diagnostic performance than both chest radiography and TTE imaging for the assessment of cardiac lead perforation.*

**Keywords** Heart injury · Radiography · Echocardiography · Tomography, x-ray computed

**Abbreviations**

| | |
|---|---|
| AUROC | Area under the receiver-operating characteristic curve |
| ECG | Electrocardiography |
| MPR | Multiplanar reformation |
| NPV | Negative predictive value |
| PACS | Picture-archiving and communication system |
| PPV | Positive predictive value |

Xiang Zhang and Chushan Zheng contributed equally to this work.

✉ Jun Shen
shenjun@mail.sysu.edu.cn

[1] Department of Radiology, Sun Yat-Sen Memorial Hospital, Sun Yat-Sen University, No. 107 Yanjiang Road West, Guangzhou 510120, People's Republic of China

[2] Department of Cardiovascular Medicine, Sun Yat-Sen Memorial Hospital, Sun Yat-Sen University, No. 107 Yanjiang Road West, Guangzhou 510120, People's Republic of China

[3] Guangdong Provincial Key Laboratory of Electrocardio Physiology and Arrhythmia, Sun Yat-Sen Memorial Hospital, Sun Yat-Sen University, No. 107 Yanjiang Road West, Guangzhou 510120, People's Republic of China

ROC Receiver-operating characteristic curve
ROI Region of interest
TTE Transthoracic echocardiography

## Introduction

Implantation of cardiac devices, such as pacemakers, implantable cardioverter defibrillators and cardiac resynchronization therapy are the most common cardiac electrophysiological procedures [1–3] used for the treatment of many patients with cardiac arrhythmias, recurrent ventricular dysrhythmias [4] and a small proportion of patients with heart failure [2, 5]. However, a variety of implantation complications, including lead perforation, infection, erosion of the pulse generator or lead connections, and subclavian vein thrombosis, rarely occur [6]. Among them, cardiac lead perforation is a rare but potentially life-threatening complication with an incidence < 1% [7, 8]. The cardiac leads could perforate the myocardium, even reach the pericardium cavity or chest wall, which might result in fatal complications such as malignant arrhythmia and acute pericardial tamponade. The clinical management of lead perforation mainly involves simple repositioning of the lead. Other strategies including open chest lead extraction and percutaneous transvenous lead extraction might be needed, particularly when uncontrolled bleeding occurs or a lead penetrates outside the pericardium with potential risk of vascular or pulmonary damage [8].

Lead perforation is mainly identified according to clinical manifestations, programmability parameters at device interrogation or using imaging modalities, such as chest radiography, transthoracic echocardiography (TTE) and cardiac CT. Lead perforation is often accompanied by symptoms such as chest pain, dyspnea and cardiac arrest or may be clinically insidious [9]. Abnormality in programmability parameters at device interrogation might be the first diagnostic clue to cardiac lead perforation, however suffering from poor specificity [10]. Chest radiography and TTE also have poor sensitivity (27.8% and 41.2%, respectively) for the diagnosis of lead perforation [7]. Beam hardening and motion artifacts from the high-density metallic leads remain problems inherent to CT [11]. The artifacts at the lead tip will potentially lead to over- or underestimation of a subtle lead perforation [11].

Electrocardiography (ECG)-gated cardiac CT imaging allows a more accurate evaluation of the lead tip position and improved assessment of perforation because of reduced motion artifacts from metallic leads [11–13]. Case reports have described the use of chest radiography, TTE or conventional cardiac CT in the diagnosis of lead perforation [14–19]. However, to the best of our knowledge, data on the diagnostic performance of ECG-gated contrast-enhanced cardiac CT for the assessment of lead perforation are scarce.

In this study, chest radiography, TTE and ECG-gated contrast-enhanced cardiac CT images from 52 patients with clinically suspected cardiac lead perforation were retrospectively analyzed. The diagnostic sensitivity, specificity, accuracy, positive predictive value (PPV) and negative predictive values (NPV) of chest radiography, TTE and ECG-gated contrast-enhanced cardiac CT for detecting cardiac lead perforations were compared.

## Materials and methods

### Patients

This retrospective study was approved by the ethics review board of Sun Yat-Sen Memorial Hospital at Sun Yat-Sen University (Guangzhou, China), and the need to obtain informed consent was waived. Between May 2010 and Oct 2017, 2731 patients received cardiac device implantation at our institution. Among them, 52 patients who were clinically suspected of a cardiac lead perforation due to presenting symptoms (chest pain, $n$ = 17; diaphragma subsultus, $n$ = 4; oppression in chest, $n$ = 4; dyspnea, $n$ = 4), abnormal electrophysiological parameters at device interrogation ($n$ = 17) or both ($n$ = 6) were enrolled in this study. All 52 patients underwent chest radiography, TTE and ECG-gated contrast-enhanced cardiac CT examinations within 3 days to identify the lead perforation. Among 52 patients, 13 were diagnosed with lead perforation (lead perforation group). Four patients had their diagnosis confirmed by open chest lead extraction surgery and nine by normal electrophysiological parameters at device interrogation after lead repositioning. The remaining 39 patients were diagnosed without lead perforation (lead non-perforation group). This diagnosis was determined by an expert panel consisting of three cardiovascular physicians (B.H., P.L. and J.W. with 7, 15 and 25 years of experience with cardiac device operation and diagnosis of cardiovascular disease, respectively). After a comprehensive review of the clinical follow-up data including symptoms, electrophysiological parameters at device interrogation and TTE [7], the absence of lead perforation was identified in these 39 patients according to a rapid disappearance of symptoms, normal electrophysiological parameters at device interrogation during a short-time follow-up (range: 1 to 5 days; median: 3 days) after conservative treatment and negative TTE imaging on follow-up (range: 1 to 5 days; median: 2 days). Thus, a composite reference standard of surgical and electrophysiological results and clinical follow-up was used to determine the diagnostic performance of chest radiography, TTE and ECG-gated contrast-enhanced cardiac CT. For all 52 patients who were suspected of having cardiac lead perforation, demographic data, including the indication of cardiac device implantation, device type, lead type, perforation time after implantation,

clinical symptom, electrical parameters at device interrogation and treatment, were recorded.

## Chest radiography and evaluation

Posteroanterior and lateral chest radiography was performed using a digital radiography system (AXIOM Aristos VX; Siemens Healthineers) in each patient during a full-inspiratory breath-hold. The parameters were as follows: a voltage of 125 kV, tube current of 200 mA and automatic exposure control. The obtained chest images were independently reviewed by two radiologists (C.Z. and J.S., with 5 and 17 years of experience with diagnostic imaging of cardiovascular disease, respectively) on a picture-archiving and communication system (PACS, Centricity RA1000 Workstation V.3.0; GE Healthcare). Any disagreements were resolved by consensus. The two reviewers were blinded to the TTE and ECG-gated contrast-enhanced cardiac CT images. Lead perforation was considered present when a lead tip extended more than 2 mm beyond the cardiac contour or a lead tip forward movement was identified compared with the chest radiography performed soon after the initial cardiac device implantation, as previously described [7, 8, 19, 20]. If a lead perforation was identified, the perforated location was recorded.

## Transthoracic echocardiogram and evaluation

TTE examination was performed using an ultrasound machine (Vivid E9; GE Healthcare). Patients were examined in supine position with quiet respiration or while holding their breath. The standard parasternal long- and short-axis views, modified right ventricle inlet tract view and apical four-, two- and three-chamber views were used to assess lead perforation. Dedicated apical right ventricular views and subcostal views were also obtained. TTE images were independently reviewed and evaluated by two ultrasound doctors (P.W. and S.Z., with 5 and 13 years of experience in ultrasonic diagnosis of cardiovascular disease, respectively) with PACS (Centricity RA1000 Workstation V.3.0; GE Healthcare). Any discrepancies were resolved by consensus. The two reviewers were blinded to the chest radiography and ECG-gated cardiac CT images. Lead perforation was identified when a lead tip extended more than 2 mm beyond the outer margin of the myocardium, as previously described [7]. If a lead perforation was considered present, the perforated location, lead tip position and pericardial effusion were recorded.

## Electrocardiography-gated contrast-enhanced cardiac CT and image evaluation

ECG-gated contrast-enhanced cardiac CT imaging was performed using a 64-slice CT scanner (Somatom Sensation 64; Siemens Healthineers) with a retrospective ECG-gated technique. All patients were scanned craniocaudally in the supine position, and the bilateral arms were elevated in close contact with the head. All the patients received respiratory training by a technician (H.H., with 12 years of experience in ECG-gated cardiac CT scanning), and their heart rates were monitored. The heart rates of 52 patients during CT examination ranged from 47 to 77 beats/min (median, 63 beats/min). None of the patients received medication to control heart rates. In the absence of contraindications (hypotension, severe anemia, current use of nitrate medications, known nitroglycerin allergy), patients were given a 0.5-mg nitroglycerin tablet (Peking Yimin Pharmaceutical Co., Ltd) sublingually 2 min before scanning. The contrast-enhanced images were obtained after intravenous injection of iodinated nonionic contrast agent (Iohexol; 350 mg/dl iodine, GE Healthcare) with a speed of 5 ml/s at a dose of 1.0 ml/kg body weight, followed by the injection of 50 ml saline at the same speed using a dual-head injector (Medrad Stellant CT injector System; Medrad Inc). Automatic bolus-tracking technology was used. The region of interest (ROI) was set at the descending aorta of the aorto-pulmonary fenestration plane, and the triggering threshold value was 100 Hounsfield units. The patients held their breaths as soon as contrast material in the ROI reached the threshold, and the contrasted-enhanced scan was started 5 s later. The scan range included the whole heart from the superior border of the aortic arch to the diaphragmatic surface of the heart. The scan parameters were as follows: a voltage of 120 kV, tube current of 550 mAs, rotation time of 0.35 s and DFOV of 25 cm. The CT dose index was 65.61 ± 5.1 mGy.

The CT raw data were reconstructed into thin slice images with a 0.6-mm slice thickness and 0.4-mm reconstruction increment using a B46f soft-tissue kernel on a CT workstation (AW 4.6, GE Healthcare). The "best diastolic" phase images, on which the metallic and motion artifacts of the electrode cable were mildest, were selected from serial 66%-86% R-R interval images to be used for assessment, as previously described [12]. These "best diastolic" phase images were post-processed by using a multiplanar reformation (MPR) technique by one radiologist (X.Z., with 7 years of experience with cardiac CT reformation) to display the orientation of the electrode and location of the lead tip. The oblique axial or oblique coronal images along the long axis of the electrode wires inside the ventricles were obtained to depict the relationship among the lead tip, myocardium and pericardium.

ECG-gated contrast-enhanced cardiac CT images were independently reviewed by two radiologists (X.D. and G.L., with 10 and 25 years of experience with vascular disease diagnosis, respectively) with PACS (Centricity RA1000 Workstation V.3.0; GE Healthcare). Any disagreements were resolved by consensus. The image window level and window width could be adjusted freely to minimize beam-hardening artifacts to

depict the cardiac and lead structures. The two reviewers were blinded to the chest radiography and TTE images. The presence of perforation was identified when a lead tip extended more than 2 mm beyond the interface of the blood pool and myocardium-epicardial fat, as previously described [12]. If a lead perforation was present, the perforated location, lead tip position and pericardial effusion were recorded.

### Statistical analysis

Agreement on the imaging evaluation between the two readers was assessed with the Cohen $\kappa$ statistic. The normality of the distribution of continuous variables was determined by using Shapiro-Wilk's test. Continuous variables were expressed as the mean ± standard deviation if they conformed to a normal distribution and otherwise were expressed as range and median. Categorical variables were presented as numbers or percentages. For comparison between the perforation and non-perforation groups, the continuous variables conforming to the normal distribution (patient age, body mass index, NYHA class and ejection fraction) were compared by *t*-tests. The categorical variables (patient gender, clinical symptom and device type) were compared by $\chi^2$ test. The sensitivity, specificity, accuracy, PPV and NPV were calculated for chest radiography, TTE and ECG-gated contrast-enhanced cardiac CT using the reference standard described earlier. The diagnostic performances of these three modalities were evaluated by receiver-operating characteristic curves (ROCs). The area under the ROCs (AUROCs) were compared by using the McNemar test. All statistical analyses were performed using SPSS, and $p < 0.05$ was considered a statistically significant difference.

## Results

### Demographics and clinical features

The clinical characteristics of the 52 patients are listed in Table 1. Among 101 leads implanted in 52 patients, 64 leads (64/101, 63.4%) were placed in the right ventricle, and the remaining 37 leads (37/101, 36.6%) were placed in the right atrium. Thirteen leads (13/101, 12.9%) in 13 patients (13/52, 25%) were confirmed as cardiac lead perforation. There were no significant differences in the age, gender, ejection fraction, New York Heart Association (NYHA) class, body mass index (BMI), clinical symptom or device type between the lead perforation and non-perforation patients. Twenty-six patients without lead perforation (Fig. 1) had clinical symptoms including dyspnea ($n = 13$), chest pain ($n = 11$) and palpitation ($n = 2$).

The clinical data from the 13 patients with lead perforation are listed in Table 2. All the leads were active-fixation electrodes. Six patients (6/13, 46.2%) had acute lead perforation (less than 1 month after cardiac lead implantation), and the remaining seven patients (7/13, 53.8%) had chronic lead perforation (1 or more months after cardiac lead implantation). Four patients (4/13, 30.8%) were asymptomatic, three patients (3/13, 23.1%) had chest pain, three patients (3/13, 23.1%) had dyspnea, two patients (2/13, 15.4%) had diaphragm subsultus,

**Table 1** Clinical characteristics of 52 patients

| Characteristic | Patients ($n = 52$) | Patient with lead perforation ($n = 13$) | Patient without lead perforation ($n = 39$) | *p* value* |
|---|---|---|---|---|
| Age (years), mean ± SD | 71.8 ± 9.5 | 72.5 ± 9.0 | 71.2 ± 9.8 | 0.691 |
| Gender | | | | 1.000 |
| Male | 23 | 6 | 17 | |
| Female | 29 | 7 | 22 | |
| Ejection fraction (%) mean ± SD | 59.9 ± 16.1 | 61.5 ± 15.8 | 58.3 ± 16.3 | 0.539 |
| NYHA class mean ± SD | 2.7 ± 0.7 | 2.9 ± 0.8 | 2.6 ± 0.7 | 0.158 |
| BMI ($kg/m^2$) mean ± SD | 26.1 ± 3.7 | 26.0 ± 3.7 | 26.2 ± 3.6 | 0.868 |
| Clinical symptoms | | | | 1.000 |
| Present | 35 | 9 | 26 | |
| Absent | 17 | 4 | 13 | |
| Device type | | | | 0.909 |
| DC PM | 30 | 9 | 21 | |
| SC PM | 6 | 1 | 5 | |
| DC ICD | 13 | 3 | 10 | |
| CRT | 3 | 0 | 3 | |

Note: SD = standard deviation; NYHA = New York Heart Association; BMI = body mass index; DC = dual chamber; PM = pacemaker; SC =single chamber; ICD = implantable cardiac defibrillator; CRT = cardiac resynchronization therapy. *The difference between patients with lead perforation and non-perforation

and one patient (1/13, 7.7%) had oppression in the chest. Nine patients (9/13, 69.2%) were treated with lead repositioning, and four patients (4/13, 30.8%) were treated by open chest lead extraction.

## Imaging features of lead perforation

The imaging features of 13 patients with lead perforation are listed in Table 3 (Fig. 2, 3, 4, and 5). Lead perforation occurred at the right ventricular apex (9/13, 69.2%) and anteroinferior wall (4/13, 31.8%). The perforated lead tip frequently extended beyond the pericardium (10/13, 76.9%), and three patients had a lead tip located in the pericardial cavity (3/13, 23.1%). Most patients (10/13, 76.9%) had a pericardial effusion.

## Diagnostic performance of chest radiography, TTE and cardiac CT

The $\kappa$ values between the two readers were 0.833 for chest radiographic evaluation, 0.902 for transthoracic echocardiogram evaluation and 0.902 for ECG-gated contrast-enhanced cardiac CT evaluation. The interobserver agreement of the imaging evaluation was good.

The diagnostic performances of chest radiology, TTE and ECG-gated contrast-enhanced cardiac CT are listed in Table 4. When a composite reference standard of surgical and electrophysiological results and clinical follow-up was used, ECG-gated contrast-enhanced cardiac CT imaging had a higher sensitivity, specificity, accuracy, PPV and NPV for the

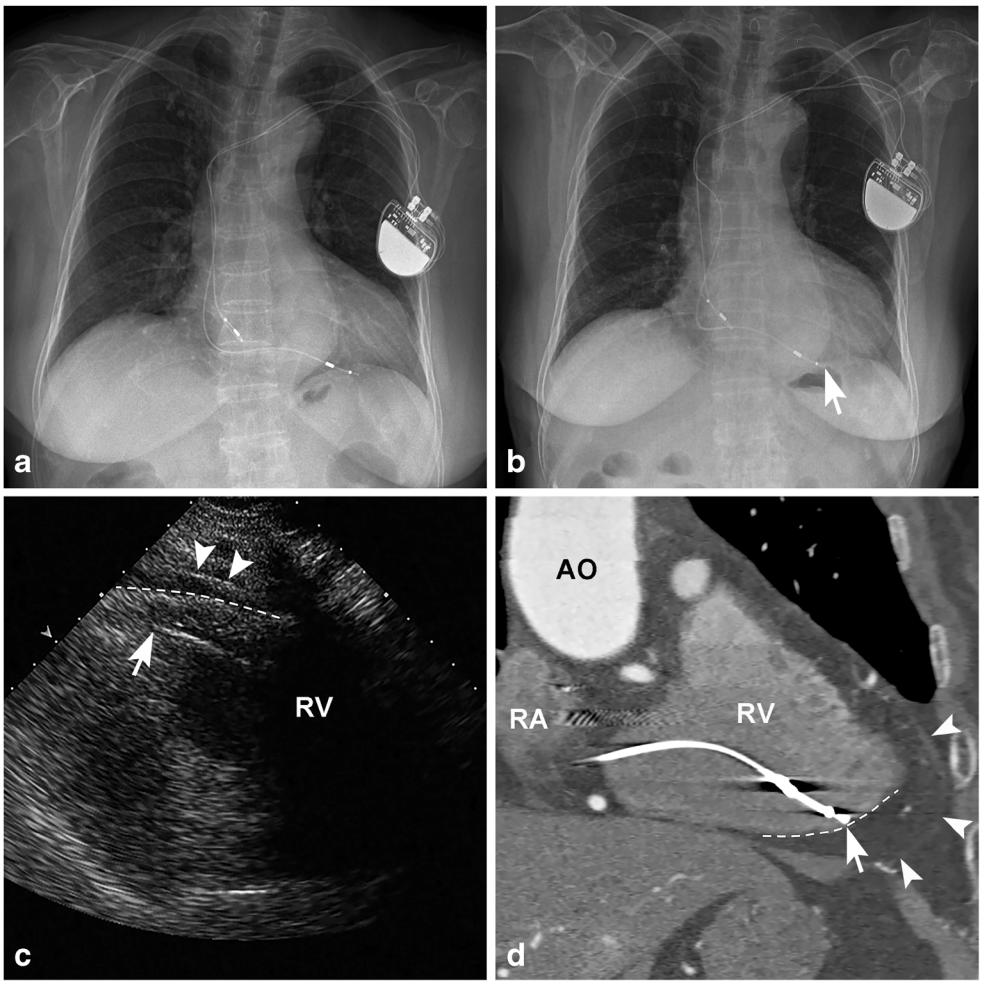


**Fig. 1** Non-perforated right ventricular pacemaker lead. (**a**) Posteroanterior chest radiograph obtained immediately after initial implantation showing the position of dual-chamber pacemaker leads. (**b**) Posteroanterior chest radiograph when suspicious for lead perforation showing no obvious change in the position of the right ventricular lead tip (arrow), and the right ventricular lead tip (arrow) is located in the normal position without extending beyond the cardiac contour. (**c**) Modified right ventricle inlet tract view of the transthoracic echocardiogram shows that the right ventricular lead tip (arrow) is located in the myocardium without extending beyond the outer margin of myocardium (white dashed line). The pericardium (arrowhead) is clearly displayed. (**d**) Oblique coronal MPR image of ECG-gated contrast-enhanced cardiac CT shows the architecture and the position of the right ventricular lead tip (arrow), which is located in the right ventricle anteroinferior wall without extending beyond the interface of the blood pool and myocardium-epicardial fat (white dashed line). The pericardium (arrowhead) is clearly depicted. RV = right ventricle; RA = right atrium; AO = arteria aorta; MPR = multiplanar reformation; ECG = electrocardiography

**Table 2** Clinical data of 13 patients with cardiac lead perforation

| Patient | Gender | Age (years) | Indication of cardiac device implantation | Device type | Lead type | Perforation time after implantation | Clinical symptom | Device interrogation parameter | Treatment |
|---|---|---|---|---|---|---|---|---|---|
| 1 | F | 76 | AF with slow ventricular rate | DC PM | Active | 9 days | Diaphragm subsultus | Pacing threshold↑, impedance abnormality | Reposition |
| 2 | F | 63 | SSS | DC PM | Active | 6 days | Chest pain | Loss of capture | Reposition |
| 3 | M | 76 | AF with slow ventricular rate | SC PM | Active | 6 months | Chest pain | Sensing abnormality | Reposition |
| 4 | M | 83 | SSS | DC PM | Active | 7 years | None | Pacing threshold↑, impedance abnormality | Open chest lead extraction |
| 5 | M | 87 | SSS | DC PM | Active | 7 days | None | Pacing threshold↑, impedance abnormalitiy | Reposition |
| 6 | M | 60 | SSS | DC PM | Active | 1 year | None | Normal | Reposition |
| 7 | F | 65 | CD | DC ICD | Active | 4 months | Diaphragm subsultus | Loss of capture | Open chest lead extraction |
| 8 | F | 70 | SSS | DC PM | Active | 25 days | Dyspnea | Normal | Reposition |
| 9 | F | 74 | SSS | DC PM | Active | 28 days | Chest pain | Impedance abnormality | Reposition |
| 10 | F | 79 | SSS | DC PM | Active | 8 months | Dyspnea | Pacing threshold↑, impedance abnormality | Open chest lead extraction |
| 11 | F | 69 | III° AVB | DC PM | Active | 1 year | Oppression in chest | Normal | Reposition |
| 12 | M | 81 | DCM | DC ICD | Active | 17 days | Dyspnea | Loss of capture | Open chest lead extraction |
| 13 | M | 59 | HC | DC ICD | Active | 4 months | None | Loss of capture | Reposition |

Note: F = female; M = male; AF = atrial fibrillation; SSS = sick sinus syndrome; AVB = atrioventricular block; CD = coronary disease; DCM = dilated cardiomyopathy; HC = hypertrophic cardiomyopathy; DC = dual-chamber; PM = pacemaker; SC = single-chamber; ICD = implantable cardiac defibrillator; ↑ = Rise

diagnosis of cardiac lead perforation than chest radiography and TTE. The diagnostic accuracy of ECG-gated contrast-enhanced cardiac CT was 98.1%. Only one case was misdiagnosed as cardiac lead perforation because the lead tip

**Table 3** Imaging features of 13 patients with cardiac lead perforation

| Patient | Perforated location | | | Lead tip position | | | Pericardial effusion | | |
|---|---|---|---|---|---|---|---|---|---|
| | CR | TTE | ECG-CT* | CR | TTE | ECG-CT* | CR | TTE | ECG-CT* |
| 1 | — | RV Ai wall | RV Ai wall | — | Ep space | Ep space | — | Present | Present |
| 2 | — | — | RV Ai wall | — | — | Pc cavity | — | Present | Present |
| 3 | — | — | RV apex | — | — | Ep space | — | Present | Present |
| 4 | — | RV apex | RV apex | — | Pc cavity | Pc cavity | — | Absent | Absent |
| 5 | — | — | RV apex | — | — | Pc cavity | — | Present | Present |
| 6 | — | RV Ai wall | RV Ai wall | — | Ep space | Ep space | — | Present | Present |
| 7 | RV apex | RV apex | RV apex | — | Ep space | Ep space | — | Absent | Absent |
| 8 | — | RV Ai wall | RV Ai wall | — | Ep space | Ep space | — | Present | Present |
| 9 | RV apex | RV apex | RV apex | — | Ep space | Ep space | — | Absent | Absent |
| 10 | — | — | RV apex | — | — | Ep space | — | Present | Present |
| 11 | — | RV apex | RV apex | — | Ep space | Ep space | — | Present | Present |
| 12 | RV apex | RV apex | RV apex | — | Ep space | Ep space | — | Present | Present |
| 13 | — | RV apex | RV apex | — | Ep space | Ep space | — | Present | Present |

Note: CR = chest radiography; TTE = transthoracic echocardiogram; ECG-CT = electrocardiography-gated contrast-enhanced cardiac computed tomography; RV = right ventricle; Ai = anteroinferior; Ep = extrapericardial; Pc = Pericardial; *both transverse sectional CT images and multiplanar reformatted images are available. —: Negative results or unable to evaluate

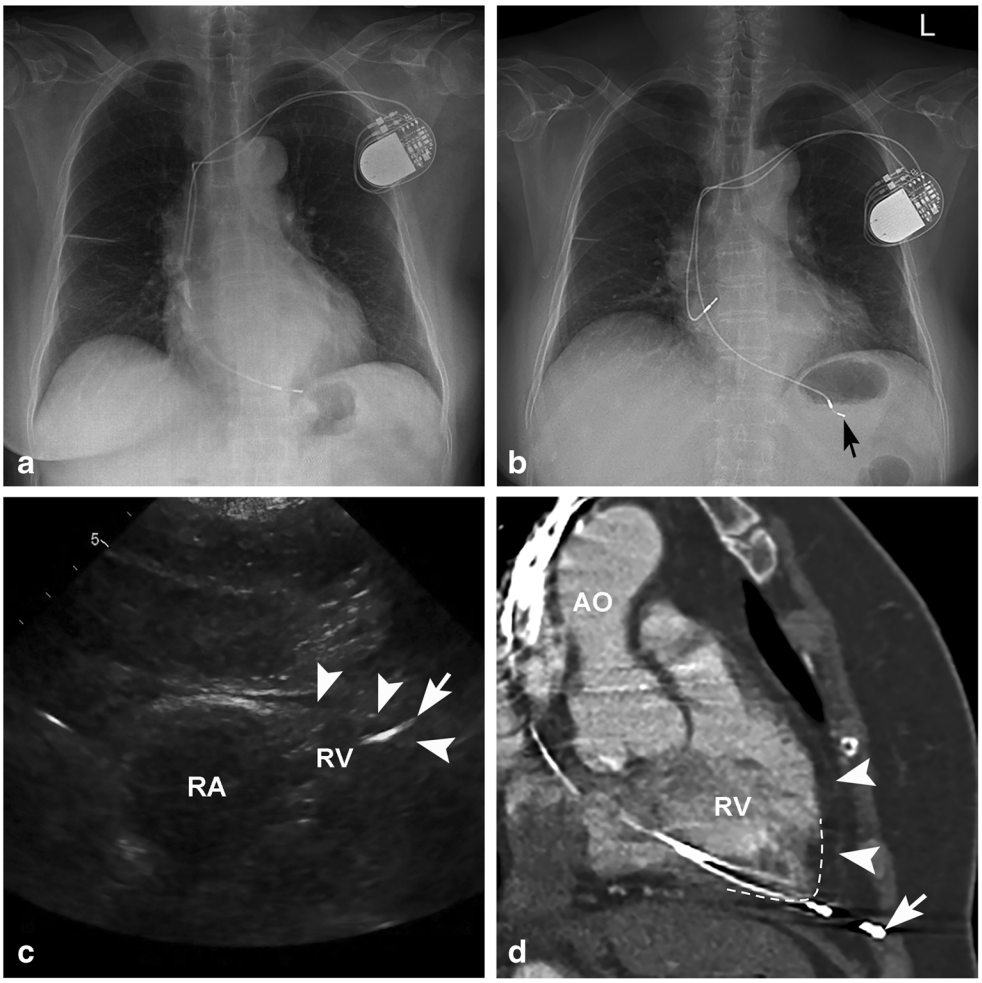


**Fig. 2** Perforated right ventricular pacemaker lead in case 9. (**a**) Posteroanterior chest radiograph showing the position of dual-chamber pacemaker leads immediately after initial implantation. (**b**) Posteroanterior chest radiograph when suspicious of lead perforation showing a movement of the right ventricular lead tip (arrow) position compared with the chest radiograph immediately after initial implantation, and the right ventricular lead tip (arrow) extends beyond the cardiac contour. (**c**) Modified right ventricle inlet tract view of transthoracic echocardiogram showing that the right ventricular lead (arrow) perforates the pericardium (arrowhead) of the right ventricular apex, and the lead tip is located in the extrapericardial space. (**d**) Oblique coronal MPR image of ECG-gated contrast-enhanced cardiac CT showing that the right ventricular lead perforates through the pericardium (arrowhead) of the right ventricular apex, and the lead tip is located in the chest wall (arrow). The interface of the blood pool and myocardium-epicardial fat (white dashed line) is clearly shown. RV = right ventricle; RA = right atrium; AO = arteria aorta; MPR = multiplanar reformation; ECG = electrocardiography

crossed nearly but < 2 mm beyond the interface of the blood pool and myocardium-epicardial fat. The AUROC of ECG-gated contrast-enhanced cardiac CT was higher than those of chest radiography and TTE ($p < 0.001$, Fig. 6).

## Discussion

In our study, when a composite reference standard of surgical and electrophysiological results and clinical follow-up was used, ECG-gated contrast-enhanced cardiac CT had a higher sensitivity, specificity, accuracy, PPV and NPV than chest radiography and TTE for the diagnosis of cardiac lead perforation. ECG-gated contrast-enhanced cardiac CT had a diagnostic accuracy of 98.1%.

Chest radiography has often been used to evaluate lead perforation in the last decade [4, 20]. However, only obvious lead perforation such as penetrating the ventricle free wall and terminating in the chest wall can be detected by chest radiography [21]. Because chest radiography can hardly show the structures of the myocardium and pericardium, it provides limited information on the depth of lead penetration into the myocardium or pericardium. Chest radiography has been reported to be an inaccurate method for identifying lead perforation and demonstrates poor diagnostic sensitivity (15%) and interobserver agreement ($\kappa$ = -0.1) [12]. In our study, chest radiography had the lowest sensitivity (38.5%), lower than that of TTE (69.2%) and ECG-gated contrast cardiac CT (100%). Other than chest radiography, TTE is commonly used for the diagnosis of lead perforation because it can provide

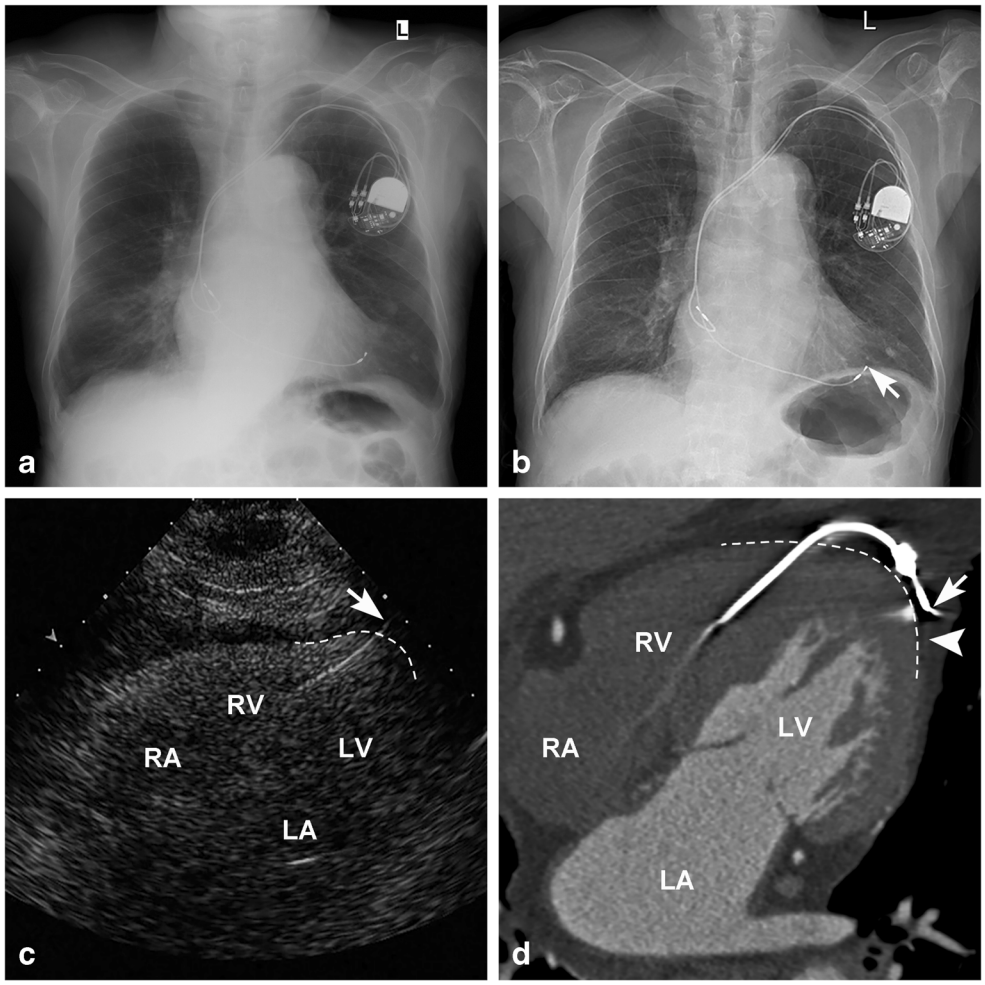


**Fig. 3** Perforated right ventricular pacemaker lead in case 4. (**a**) Posteroanterior chest radiograph showing the position of dual-chamber pacemaker leads immediately after initial implantation. (**b**) Posteroanterior chest radiograph when suspicious of lead perforation showing no obvious movement of right ventricular lead tip (arrow) position compared with the chest radiograph immediately after initial implantation, and the ventricular pacemaker lead is located in the normal position without extending beyond the cardiac contour. (**c**) Modified apical four-chamber view of the transthoracic echocardiogram showing that the right ventricular lead (arrow) perforates through the outer margin of the myocardium (white dashed line) of the right ventricular apex, but the hook-like lead tip cannot be seen in this view because of the limitation of the acoustic window. (**d**) Oblique axial MPR image of ECG-gated contrast-enhanced cardiac CT showing that the right ventricular lead perforates through the interface of the blood pool and myocardium-epicardial fat (white dashed line) of the right ventricular apex. The lead tip (arrow) is located close to the pericardium (arrowhead). LV = left ventricle; LA = left atrium; RV = right ventricle; RA = right atrium; MPR = multiplanar reformation; ECG = electrocardiography

clear visualization of the lead tip and pericardial effusion [7]. TTE reportedly has a high specificity (84.2%) but poor sensitivity (41.2%) [7]. In our study, TTE had a moderate sensitivity (69.2%) and high specificity (87.2%). The use of conventional cardiac CT can improve the diagnostic specificity (85.7%) and sensitivity (100%) [7]. Although CT may be a useful imaging modality, its diagnostic performance is limited by the presence of metallic streak artifacts [8]. The artifacts at the lead tip potentially result in over- or underestimation with subtle lead perforation [11]. ECG-gated cardiac CT is expected to have potential benefits for precise identification of the position of the lead tip since it could reduce the effect of beam hardening and motion artifacts [11–13]. In our study, the diagnostic capacity of ECG-gated contrast-enhanced cardiac CT imaging was high with a sensitivity of 100%, specificity of 97.4% and accuracy of 98.1%. The interface between the cardiac cavity and myocardium could be better discriminated on contrast-enhanced images, which is beneficial for the clear detection of the relationship between the lead tip and myocardium. In addition, the use of MPR images could aid in demonstrating the lead tip configuration and increasing confidence in the assessment of the tip position [12]. In our study, the structures of the pericardium and myocardium-epicardial fat interface, which are the key anatomical markers for diagnosing lead perforation, were clearly discernible on ECG-gated contrast-enhanced cardiac CT images, and the relationship between these structures and the lead tip was clearly shown on MPR images.

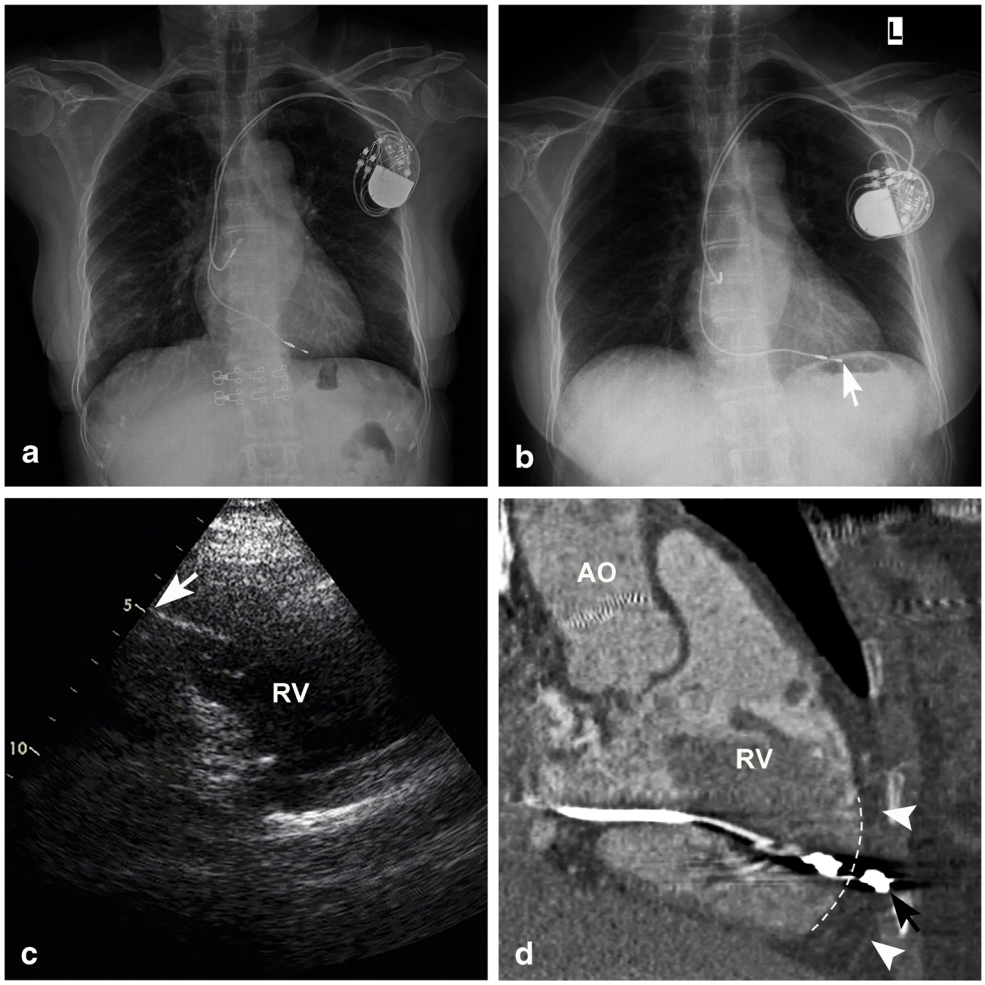


**Fig. 4** Perforated right ventricular pacemaker lead in case 2. (**a**) Posteroanterior chest radiograph showing the position of dual-chamber pacemaker leads immediately after initial implantation. (**b**) Posteroanterior chest radiograph in the posteroanterior view when suspicious for lead perforation showing a movement of the right ventricular lead tip (arrow) position compared with the chest radiograph immediately after initial implantation, but the right ventricular lead tip (arrow) is in the normal position without extending beyond the cardiac contour. (**c**) Dedicated apical right ventricular view of the transthoracic echocardiogram showing the location of the right ventricular lead tip (arrow), which appears to be in the normal position. (**d**) Oblique coronal MPR image of ECG-gated contrast-enhanced cardiac CT showing that the right ventricular lead tip (black arrow) perforates the interface of the blood pool and myocardium-epicardial fat (white dashed line) of the right ventricle anteroinferior wall. The lead tip (arrow) is located close to the pericardium (white arrowhead). RV = right ventricle; AO = arteria aorta; MPR = multiplanar reformation; ECG = electrocardiography

There are limitations to our study. First, our results are based on a small patient population because of the low incidence of cardiac lead perforation. A larger multicenter study might be required to further validate the value of ECG-gated cardiac CT for detecting cardiac lead perforation. Second, a composite reference standard of surgical and electrophysiological results and clinical follow-up was used. In particular, the absence of lead perforation in 39 patients was assessed by an expert panel consisting of three cardiovascular physicians who were not previously involved in imaging analysis in our study. The diagnosis was made according to short-term clinical follow-up data. To date, there is no an established gold standard for diagnosing lead perforation. Direct thoracotomy or thoracoscopy or normal electrophysiological parameters at device interrogation after lead repositioning can be used to confirm the lead perforation. However, it is impossible for patients who were suspected to have lead non-perforation to accept an open chest surgery or thoracoscopy to confirm the diagnosis. Clinically, these patients are treated with close follow-up. Thus, it is reasonable that the diagnosis of 39 patients without lead perforation was determined according to a short-term clinical follow-up. Additionally, a cardiac perforation is probably not healed in a short time, such as 5 days. Third, only a single-phase contrast-enhanced ECG-gated cardiac CT was performed. Other examination strategies such as dual-phase contrast-enhanced ECG-gated contrast-enhanced cardiac CT and prospective ECG-gated cardiac CT scans were not attempted. The use of dual-phase contrast-enhanced imaging would increase the dosage of ionizing radiation in the same patient. Indeed, the radiation dosage from a prospective ECG-gated cardiac CT scan is substantially lower than that of a

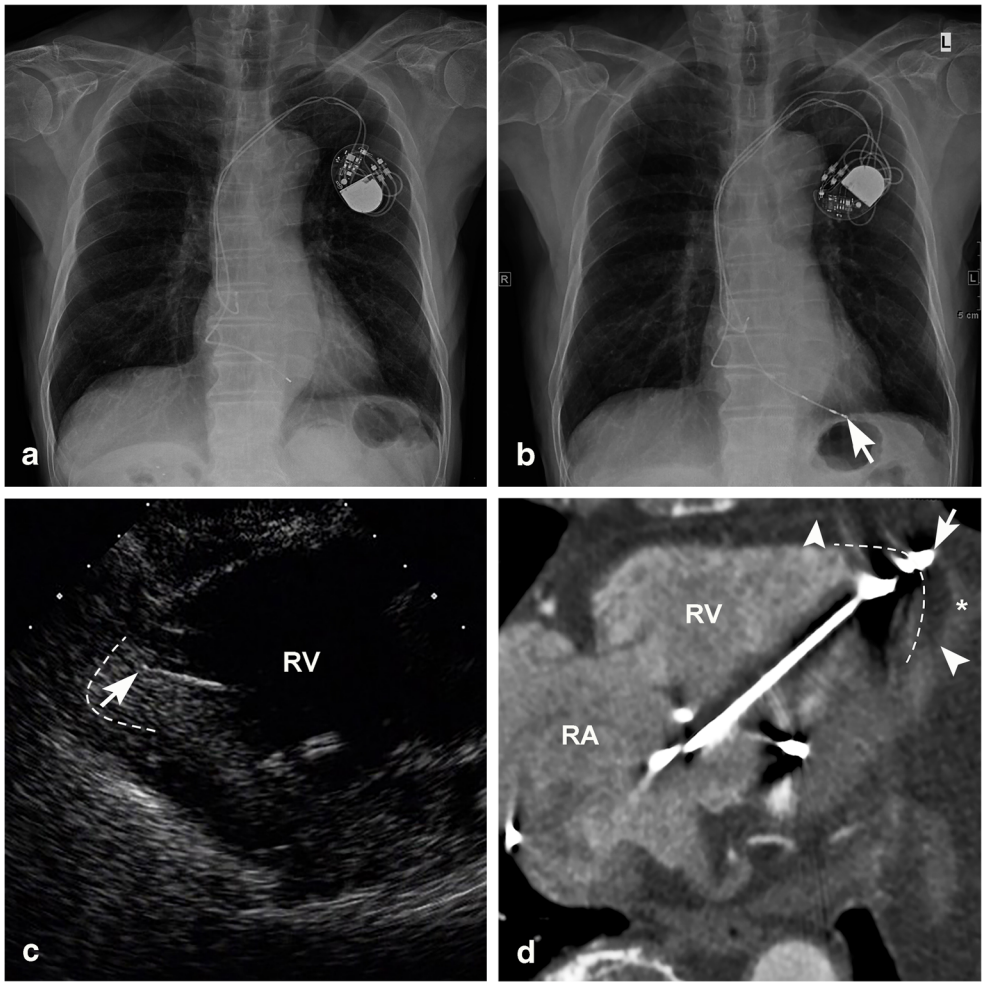


**Fig. 5** Perforated right ventricular pacemaker lead in case 5. (**a**) Posteroanterior chest radiograph showing the position of dual-chamber pacemaker leads immediately after initial implantation. (**b**) Posteroanterior chest radiograph when suspicious for lead perforation showing a movement of the right ventricular lead tip (arrow) position compared with the chest radiograph immediately after initial implantation, but the right ventricular pacer lead tip (arrow) is in the normal position without extending beyond the cardiac contour. (**c**) Dedicated apical right ventricular view from the transthoracic echocardiogram showing the right ventricular pacer lead tip (arrow), which appears to be within the region of the outer margin of the myocardium (white dashed line). (**d**) Oblique axial MPR image of ECG-gated contrast-enhanced cardiac CT showing that the right ventricular pacer lead tip (arrow) perforates through the interface of the blood pool and myocardium-epicardial fat (white dashed line) and is located close to the pericardium (arrowhead) of the right ventricular apex. Pericardial effusion was seen in the pericardial cavity of the right ventricular apex (asterisk). RV = right ventricle; RA = right atrium; MPR = multiplanar reformation; ECG = electrocardiography

**Table 4** Diagnostic performance of chest radiography, TTE and ECG-gated contrast-enhanced cardiac CT in cardiac lead perforation

| Imaging method* | Chest radiography | TTE | ECG-gated contrast cardiac CT |
|---|---|---|---|
| No. of true positive | 5 | 9 | 13 |
| No. of false positive | 6 | 5 | 1 |
| No. of true negative | 33 | 34 | 38 |
| No. of false negative | 8 | 4 | 0 |
| Sensitivity (%) | 38.5 (15.1-67.7) | 69.2 (38.9-89.6) | 100.0 (71.7-100.0) |
| Specificity (%) | 84.6 (68.8-93.6) | 87.2 (71.8-95.2) | 97.4 (84.9-99.9) |
| Accuracy (%) | 73.1 (59.0-84.4) | 82.7 (69.7-91.8) | 98.1 (89.7-100.0) |
| PPV (%) | 45.5 (18.1-75.4) | 64.3 (35.6-86.0) | 92.9 (64.2-99.6) |
| NPV (%) | 80.5 (64.6-90.6) | 89.5 (74.3-96.6) | 100.0 (88.6-100.0) |

Note: TTE = transthoracic echocardiogram; ECG = electrocardiography; PPV = positive predicative value; NPV = negative predicative value. *Compared with a composite reference standard of surgical and electrophysiological results and clinical follow-up

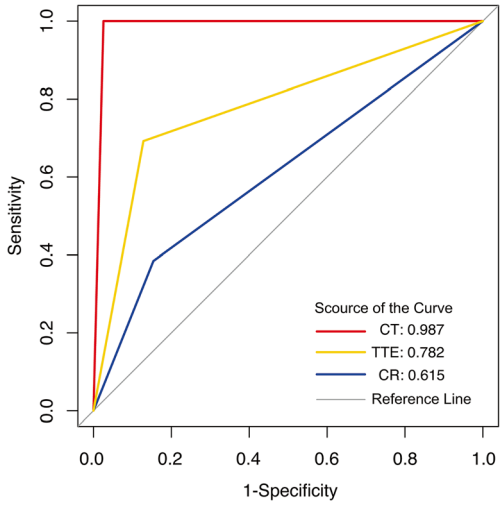


**Fig. 6** Receiver-operating characteristic curves for chest radiology, transthoracic echocardiogram and electrocardiography-gated contrast-enhanced cardiac CT in the diagnosis of cardiac lead perforation using a composite reference standard of surgical and electrophysiological results and clinical follow-up. CT = electrocardiography-gated contrast-enhanced cardiac CT; TTE = transthoracic echocardiogram; CR = chest radiograph

retrospective one [12, 22]. However, retrospective ECG-gated cardiac CT scans potentially have some benefits for cardiac lead perforation. For example, the retrospective scan mode allows reconstruction of images at any desired phase of the heart cycle and the removal of image data acquired during irregular heartbeats, which are helpful for alleviating ECG misregistration and lead motion artifacts [23–25].

In conclusion, ECG-gated contrast-enhanced cardiac CT shows good diagnostic ability for cardiac lead perforation using a composite reference standard of surgical and electrophysiological results and clinical follow-up. Where chest radiography and TTE findings are equivocal for lead perforation, ECG-gated contrast-enhanced cardiac CT can be used as an alternative for the diagnosis of cardiac lead perforation. With the advantage of precise identification of the location of the lead tip, ECG-gated contrast-enhanced cardiac CT is also helpful for lead repositioning to treat lead perforation.

**Funding** This study has received funding by Guangdong Province Universities and Colleges Pearl River Scholar Funded Scheme (2017) and the Elite Young Scholars Program of Sun Yat-Sen Memorial Hospital (grant no. J201403).

## Compliance with ethical standards

**Guarantor** The scientific guarantor of this publication is Jun Shen.

**Conflict of interest** The authors of this manuscript declare no relationships with any companies, whose products or services may be related to the subject matter of the article.

**Statistics and biometry** No complex statistical methods were necessary for this paper.

**Informed consent** Written informed consent was waived by the Institutional Review Board.

**Ethical approval** Institutional Review Board approval was obtained from the Institutional Review Board of Sun Yat-Sen Memorial Hospital of Sun Yat-Sen University (Guangzhou, China).

**Methodology**
- Retrospective
- Diagnostic study
- Performed at one institution

## References

1. Todd D, Bongiorni MG, Hernandez-Madrid A et al (2014) Standards for device implantation and follow-up: personnel, equipment, and facilities: results of the European Heart Rhythm Association Survey. Europace 16:1236–1239. https://doi.org/10.1093/europace/euu209
2. European Society of Cardiology (ESC); European Heart Rhythm Association (EHRA), Brignole M et al (2013) 2013 ESC guidelines on cardiac pacing and cardiac resynchronization therapy: the task force on cardiac pacing and resynchronization therapy of the European Society of Cardiology (ESC). Developed in collaboration with the European Heart Rhythm Association (EHRA). Europace 15:1070–1118. https://doi.org/10.1093/europace/eut206
3. Epstein AE, DiMarco JP, Ellenbogen KA et al (2013) 2012 ACCF/AHA/HRS focused update incorporated into the ACCF/AHA/HRS 2008 guidelines for device-based therapy of cardiac rhythm abnormalities: a report of the American College of Cardiology Foundation/American Heart Association Task Force on Practice Guidelines and the Heart Rhythm Society. Circulation 127:e283–e352. https://doi.org/10.1161/CIR.0b013e318276ce9b
4. Burney K, Burchard F, Papouchado M, Wilde P (2004) Cardiac pacing systems and implantable cardiac defibrillators (ICDs): a radiological perspective of equipment, anatomy and complications. Clin Radiol 59:699–708. https://doi.org/10.1016/j.crad.2004.01.009
5. Boriani G, Kranig W, Donal E et al (2010) A randomized double-blind comparison of biventricular versus left ventricular stimulation for cardiac resynchronization therapy: the Biventricular versus Left Univentricular Pacing with ICD Back-up in Heart Failure Patients (B-LEFT HF) trial. Am Heart J 159:1052–1058. https://doi.org/10.1016/j.ahj.2010.03.008
6. Ellenbogen KA, Wood MA, Shepard RK (2002) Delayed complications following pacemaker implantation. Pacing Clin Electrophysiol 25:1155–1158. https://doi.org/10.1046/j.1460-9592.2002.01155.x
7. Rajkumar CA, Claridge S, Jackson T et al (2017) Diagnosis and management of iatrogenic cardiac perforation caused by pacemaker and defibrillator leads. Europace 19:1031–1037. https://doi.org/10.1093/europace/euw074
8. Refaat MM, Hashash JG, Shalaby AA (2010) Late perforation by cardiac implantable electronic device leads: clinical presentation, diagnostic clues, and management. Clin Cardiol 33:466–475. https://doi.org/10.1002/clc.20803
9. Hirschl DA, Jain VR, Spindola-Franco H, Gross JN, Haramati LB (2007) Prevalence and characterization of asymptomatic pacemaker and ICD lead perforation on CT. Pacing Clin Electrophysiol 30:28–32. https://doi.org/10.1111/j.1540-8159.2007.00575.x
10. Huang XM, Fu HX, Zhong L et al (2014) Outcomes of lead revision for myocardial perforation after cardiac implantable electronic device placement. J Cardiovasc Electrophysiol 25:1119–1124. https://doi.org/10.1111/jce.12457

11. Pang BJ, Lui EH, Joshi SB et al (2014) Pacing and implantable cardioverter defibrillator lead perforation as assessed by multiplanar reformatted ECG-gated cardiac computed tomography and clinical correlates. Pacing Clin Electrophysiol 37:537–545. https://doi.org/10.1111/pace.12307
12. Balabanoff C, Gaffney CE, Ghersin E, Okamoto Y, Carrillo R, Fishman JE (2014) Radiographic and electrocardiography-gated noncontrast cardiac CT assessment of lead perforation: modality comparison and interobserver agreement. J Cardiovasc Comput Tomogr 8:384–390. https://doi.org/10.1016/j.jcct.2014.08.004
13. Lewis RK, Pokorney SD, Greenfield RA et al (2014) Preprocedural ECG-gated computed tomography for prevention of complications during lead extraction. Pacing Clin Electrophysiol 37:1297–1305. https://doi.org/10.1111/pace.12485
14. Boxma RPJ, Kolff-Kamphuis MGM, Gevers RMM, Boulaksil M (2017) Subacute right ventricular pacemaker lead perforation: evaluation by echocardiography and cardiac CT. J Echocardiogr 15:188–190. https://doi.org/10.1007/s12574-017-0337-5
15. Jain N, Ravipati V, Kerut EK (2016) Late pacemaker lead tip perforation documented by chest CT. Echocardiography 33:1419–1421. https://doi.org/10.1111/echo.13310
16. Nichols J, Berger N, Joseph P, Datta D (2015) Subacute right ventricle perforation by pacemaker lead presenting with left hemothorax and shock. Case Rep Cardiol 2015:983930. https://doi.org/10.1155/2015/983930
17. Henrikson CA, Leng CT, Yuh DD, Brinker JA (2006) Computed tomography to assess possible cardiac lead perforation. Pacing Clin Electrophysiol 29:509–511. https://doi.org/10.1111/j.1540-8159.2006.00385.x
18. Merla R, Reddy NK, Kunapuli S, Schwarz E, Vitarelli A, Rosanio S (2007) Late right ventricular perforation and hemothorax after transvenous defibrillator lead implantation. Am J Med Sci 334:209–211. https://doi.org/10.1097/MAJ.0b013e31814254c5
19. Yoshimori A, Kobori A, Michihiro N, Furukawa Y (2011) Delayed perforation of the right ventricular wall by a single standard-caliber implantable cardioverter-defibrillator lead detected by multidetector computed tomography. Korean Circ J 41:689–691. https://doi.org/10.4070/kcj.2011.41.11.689
20. Kirchgesner T, Ghaye B, Marchandise S, Le Polain de Waroux JB, Coche E (2016) Iatrogenic cardiac perforation due to pacing lead displacement: Imaging findings. Diagn Interv Imaging 97:233–238. https://doi.org/10.1016/j.diii.2015.03.011
21. Greenberg S, Lawton J, Chen J (2005) Images in cardiovascular medicine. Right ventricular lead perforation presenting as left chest wall muscle stimulation. Circulation 111:e451–e452. https://doi.org/10.1161/CIRCULATIONAHA.104.494732
22. Lee AM, Engel LC, Shah B et al (2012) Coronary computed tomography angiography during arrhythmia: Radiation dose reduction with prospectively ECG-triggered axial and retrospectively ECG-gated helical 128-slice dual-source CT. J Cardiovasc Comput Tomogr 6:172–183. https://doi.org/10.1016/j.jcct.2012.04.003
23. Meyer M, Haubenreisser H, Schoepf UJ et al (2017) Radiation Dose Levels of Retrospectively ECG-Gated Coronary CT Angiography Using 70-kVp Tube Voltage in Patients with High or Irregular Heart Rates. Acad Radiol 24:30–37. https://doi.org/10.1016/j.acra.2016.08.004
24. Rist C, Johnson TR, Müller-Starck J et al (2009) Noninvasive coronary angiography using dual-source computed tomography in patients with atrial fibrillation. Invest Radiol 44:159–167. https://doi.org/10.1097/RLI.0b013e3181948b05
25. Wang Y, Zhang Z, Kong L et al (2008) Dual-source CT coronary angiography in patients with atrial fibrillation: comparison with single-source CT. Eur J Radiol 68:434–441. https://doi.org/10.1016/j.ejrad.2008.09.011